



RESEARCH ARTICLE

A cable-driven elbow exoskeleton with variable stiffness actuator for upper limb rehabilitation

Lei Yang , Fuhai Zhang  and Yili Fu

The State Key Laboratory of Robotics and System, Harbin Institute of Technology, Harbin, China

Corresponding author: Fuhai Zhang; Email: zfhit@hit.edu.cn

Received: 10 May 2024; **Revised:** 23 October 2024; **Accepted:** 19 November 2024

Keywords: rehabilitation robot; elbow exoskeleton; variable stiffness actuator

Abstract

Elbow, with complex physiological structure, plays an important role in upper limb motion which can be assisted with exoskeleton in rehabilitation. However, the stiffness of elbow changes while training which decline the comfort and effect of rehabilitation. Moreover, the rotation axis of elbow is changing which will cause secondary injuries. In this paper, we design an elbow exoskeleton with a variable stiffness actuator and a deviation compensation unit to assist elbow rehabilitation. Firstly, we design a variable stiffness actuator by symmetric actuation principle to adapt the change of elbow stiffness. The parameters of the variable stiffness actuator are optimized by motion simulation. Next, we design a deviation compensation unit to follow the rotation axis deviation outside the horizontal plane. The compensation area is simulated to cover the deviation. Finally, simulation and experiments are carried out to show the performance of our elbow exoskeleton. The workspace can meet the need of daily elbow motion while the variable stiffness actuator can adjust the exoskeleton stiffness as expectation.

1. Introduction

The upper limb plays an important role in daily activities. The elbow joint is an important connecting part of the upper limb, which drives and coordinates the forearm, shoulder joint, and wrist joint. Moreover, elbow motion can ensure shoulder and hand function are normal and stable. Therefore, it's of significant importance to assist patients in elbow rehabilitation training [1, 2]. In clinical practice, rehabilitation training is led by rehabilitation therapists who perform traction movements on the elbow [3]. The action is single, repeated multiple times, time-consuming, and requires long-term training. It's proved that rehabilitation robot can provide the repetitive and progressive rehabilitation for patients with upper limb disabilities [4, 5, 6]. Not only passive movement but also training of activities of daily life can be realized with the help of rehabilitation robot. Rehabilitation robots can provide long-term training and solve the problem of insufficient manpower consuming [7, 8, 9]. Exoskeleton robot has become a research hotspot recently because it can fit the motion of upper limb including elbow. As a human-machine coupling device, elbow exoskeleton robot requires high compatibility with the human body which needs to fully adapt to the physiological characteristics of the elbow joint [10]. NURSE was designed as an arm movement aid device for both right- and left-upper limb [11]. With a big workspace to conduct physical therapy or training on individuals, the device can adapt to the physiological characteristics including kids and elderly individuals, of any age and size.

Shih uses the parallel structure of the model which has three motors directly fixed on it. The position of the structural base ensures the degree of freedom while improving its accuracy and stiffness [12]. In addition, its elbow also has a counterweight block for maintaining the balance of the mechanism. Proietti designed a soft wearable robot with sensing and control system to assist patients, reducing joint backlash

and achieving sufficient anti-drive capability [13]. In addition, a crank-slider-like mechanism was used to solve the problem of shoulder misalignment. Although the directly driven elbow joint has the above advantages, the driving motor of its mechanism is directly mounted on the exoskeleton, which makes the elbow joint part too heavy. Moreover, the elbow joint of the patient is often far from the shoulder causing large inertia which not only hinders control but also brings burden to the patient.

In order to solve the problem of the distribution of exoskeleton mass mentioned above, some authors have used the method of cable-driving to remotely arrange the drivers with a proper degree of freedom (DOF). This can reduce the mass of the elbow exoskeleton, allowing for a better distribution of mass and inertia in the upper limbs [14, 15]. At the same time, cable-driving also has better flexibility and safety. Ma has a cable-driven actuator from the elbow that is introduced through the shoulder and wound around a fixed point on the wire wheel [16]. The pretension of the cable can be changed by adjusting the relative distance between the two fixed points of the cable wheel. The exoskeleton robot (CADEN-7) has an elbow joint composed of two orthogonal axes, which act directly on the elbow joint through the Bowden cable [17]. The elbow joint exoskeleton directly contacts the human body and drives joint movement. The introduction of cable can reduce the stiffness of exoskeleton to fit the motion of elbow. Series elastic actuator (SEA) is widely used in upper limb exoskeleton. The elbow joint robot developed by Taiwan Chenggong University has a certain degree of flexibility at the joints. The elbow joints are driven by linear SEA [18]. In addition, due to the fact that the driving motor itself has a worm gear and worm gear transmission, it can obtain a larger output force through a motor with a smaller mass, with good inertia, mass distribution, and self-locking. An elbow robot uses an integral flexible unit to generate flexibility through deformation caused by force, and its torque is measured by pasting strain gauges on four spokes [19]. Dežman designed an upper limb exoskeleton with active shoulder joint and a passive elbow joint. A friction modelling of the cable-driven exoskeleton is carried out for better performance [20]. Fan introduced a feedforward compensation approach for cable-driven musculoskeletal systems which can solve the problem of the distribution of exoskeleton mass [21]. CUBE² was designed for limb rehabilitation with a novel end-effector design and autotuning capabilities to enable autonomous use [22]. CUBE² can prevent temporary injuries from having lingering or permanent effects.

However, the stiffness of elbow changes in rehabilitation. The constant stiffness of SEA can't meet the need [23]. A structure of variable stiffness actuator (VSA) is introduced to adjust the stiffness of exoskeleton [24]. The elbow robot ULIX developed by Catholic University in the United States has added a variable stiffness flexible mechanism at the elbow joint, which converts linear stiffness into nonlinear increased stiffness through a series of springs [25]. However, it should be noted that the structure of VSA is often complex, with large volume and mass, making it inconvenient for patients to wear. Thus, a compact VSA structure should be designed to adjust stiffness in rehabilitation.

Due to the slight deviation of the axis of the elbow joint during rotation, the exoskeleton does not coincide with the rotation axis of the human body [26]. This will cause excessive pressure on the human-machine contact surface of the upper limbs of the human body. Moreover, it will lead to loads in other directions at the joints, causing secondary damage to the patient. Because the angle changes of the elbow joint axis are irregular and varied, the current mainstream method is to set passive degrees of freedom to make the elbow joint of the exoskeleton adaptive. Islam designed an upper limb exoskeleton with fractional sliding mode control for less excessive pressure on the human-machine contact surface [27]. Both the mechanical design and the control method can ensure the coincidence between exoskeleton and upper limb joints. A wearable exoskeleton robot was designed with a passive degree of freedom of forward and backward extension in the exoskeleton forearm to solve the problem of elbow joint displacement [28]. They optimized the human-machine contact interface and analysed the relationship between the configuration of the motion pair and the force at the human-machine interface of the arm. Also, they solved the problem of non-overlapping elbow axes by adding degrees of freedom in the human-machine interaction interface. Verdel introduced an identification-based method improving the transparency of a robotic upper limb exoskeleton. The transparency decreases the excessive pressure which provides the efficiency and safety of rehabilitation [29]. The NEUROExos carefully considered the problem of axis misalignment caused by minor movements of the elbow joint [30]. A pulley block was used at the

Table I. Feature analysis of rehabilitation robot.

Type of robot	Number of DOF	Therapy classification	Driving method	Compensation method	Reference
Hand exoskeleton	1–5 (active)	Passive training	Hybrid Cable	Soft exoskeleton	[5]
Elbow exoskeleton*	1 (active)	Active/passive	Hybrid	NA	[14]
	0–1 (passive)	Virtual training	Motor Cable	Soft exoskeleton Compensation mechanism	[4] [19] [25] [15] [24] Ours and [18] [30]
Upper limb exoskeleton	4–7 (active)	Active/passive	Motor	NA	[12] [16] [17] [20] [27]
	1–2 (passive)	Virtual training	Cable	Soft exoskeleton	[13]
Other devices	2 (active)	Home training	Cable	NA	[11] [19]

driving joint to reduce backlash and improve sensor sensitivity. However, the motion performance and stiffness control are hard to control in clinical rehabilitation. Thus, it's important to introduce deviation compensation structure to realize safe rehabilitation.

In this paper, we design an elbow exoskeleton with a variable stiffness actuator and a deviation compensation unit to assist elbow rehabilitation which is a novel design as shown in Table I. Firstly, we design a variable stiffness actuator by the physiological analysis of elbow. To maintain the stability of elbow, the stiffness of muscle changes with the increasing force. Thus, we introduce VSA structure with symmetric actuation principle to adapt the change of elbow stiffness. The parameters of the variable stiffness actuator are optimized by motion simulation. Next, we design a deviation compensation structure to follow the rotation axis deviation outside the horizontal plane. A linkage mechanism is designed to simulate the rotation deviation of elbow axis outside the horizontal plane. The deviation of elbow axis can be covered by our axis compensation unit. Finally, simulation and experiments are carried out to show the performance of our elbow exoskeleton. An experimental platform is established for motion tests of our elbow exoskeleton. As the result shows, the workspace can meet the need of the daily elbow motion while the variable stiffness actuator can adjust the exoskeleton stiffness as expected.

To provide the assistance of elbow rehabilitation with safety and efficiency by elbow exoskeleton, our paper makes the following contributions:

1. Design a variable stiffness actuator to fit the elbow stiffness change in rehabilitation.
2. Design an axis deviation compensation unit to eliminate inappropriate torque and contact force for actuation accuracy and safety guidance.

2. Variable stiffness actuator design for elbow exoskeleton

The elbow stiffness changes in rehabilitation which will cause actuation error and uncomfot. Therefore, this paper designs a variable stiffness actuator to adjust the stiffness of elbow exoskeleton. With the physiological analysis of elbow, a symmetric actuation mechanism is designed with adjustment parameters. Simulations are carried out to optimize those parameters.

2.1 Physiological analysis of elbow structure

In a single-joint system like the elbow joint (an inverted pendulum supported by a pair of muscles), the muscles cannot follow Hooke's law as a linear system. They cannot have constant stiffness in order to maintain stability of the upper limb in daily motion. In fact, the elbow will only stabilize when the stiffness of each muscle increases with impact force. Therefore, if the elbow joint is subjected to a static

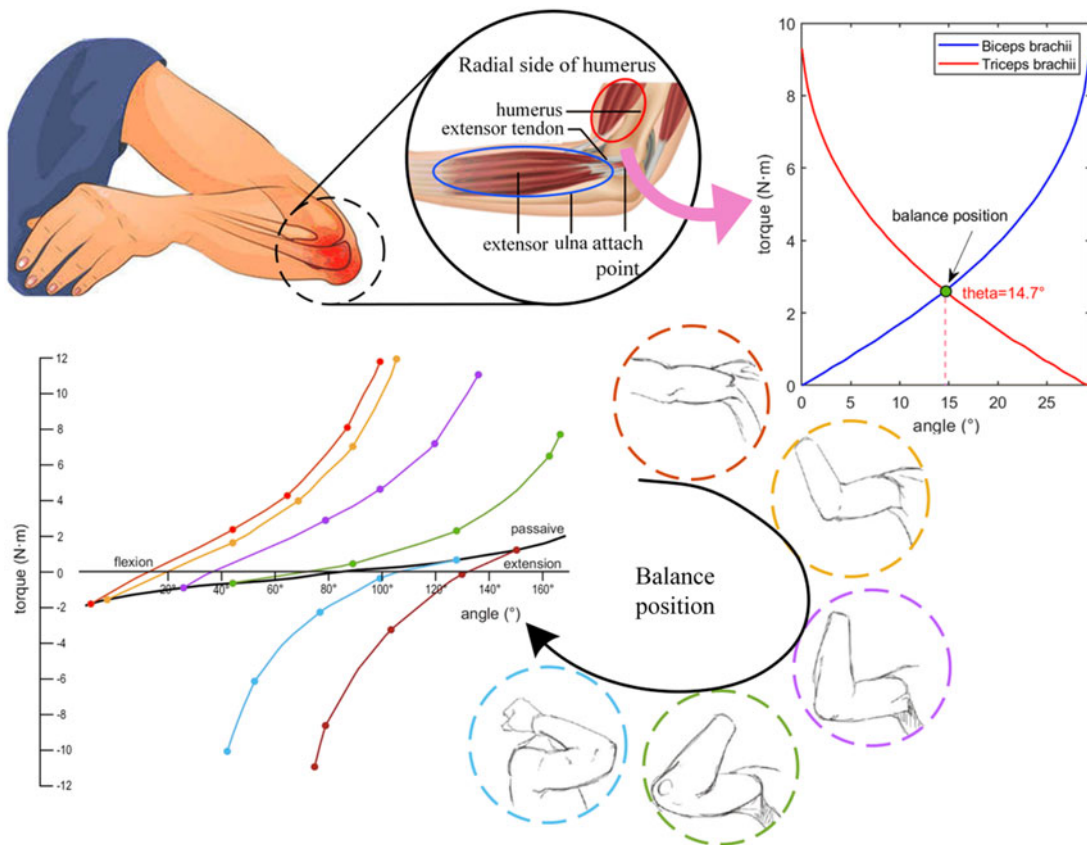


Figure 1. *Physiological analysis of elbow stiffness.*

torque load and suddenly changes the load without active human intervention, the stiffness of the muscles will increase with the magnitude of the force which is shown in Figure 1. The change of stiffness will not only cause uncomfot by collision between forearm and exoskeleton but also influence the accuracy of motion control.

With the movement of elbow, the length of humerus and extensor tendon varies around the attach point. The stiffness of upper limb will change according to Hill model. The changing stiffness of upper limb will cause disturbance in exoskeleton control. If the elbow exoskeleton only has constant stiffness, the inappropriate contact force will not be eliminated. Therefore, in the design of the actuator, a variable stiffness characteristic should be achieved to fit the change of elbow stiffness. The variable stiffness can help modify the muscle power pattern and increase the control accuracy of exoskeleton. We design a VSA mechanism which can realize specific parameter variation (usually angle or displacement). Moreover, we introduce elastic elements in VSA to transform angular variation to torque variation. The structure of VSA can adjust the stiffness of our elbow exoskeleton during rehabilitation. By optimizing the VSA structure, the stiffness variation can satisfy the need of elbow.

2.2 Principle of variable stiffness actuator

Due to the fact that the actuator of the exoskeleton mimics the antagonistic actuation of the human elbow muscles, indirect control can be achieved by controlling the antagonistic actuation relationship between left input wheel and right input wheel as shown in Figure 2. The two VSA mechanisms are located on both sides of the elbow joint. Meanwhile, the coaxial cable wheels on the left and right serve as torque

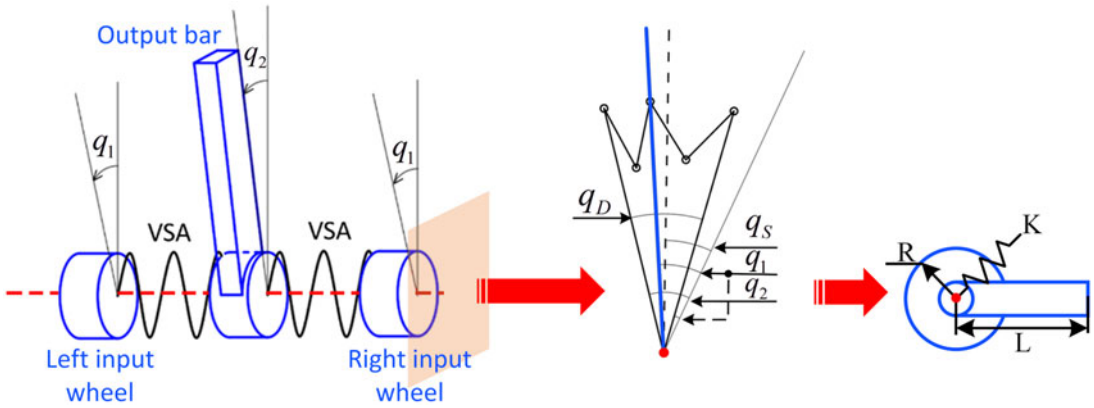


Figure 2. Symmetric principle of VSA.

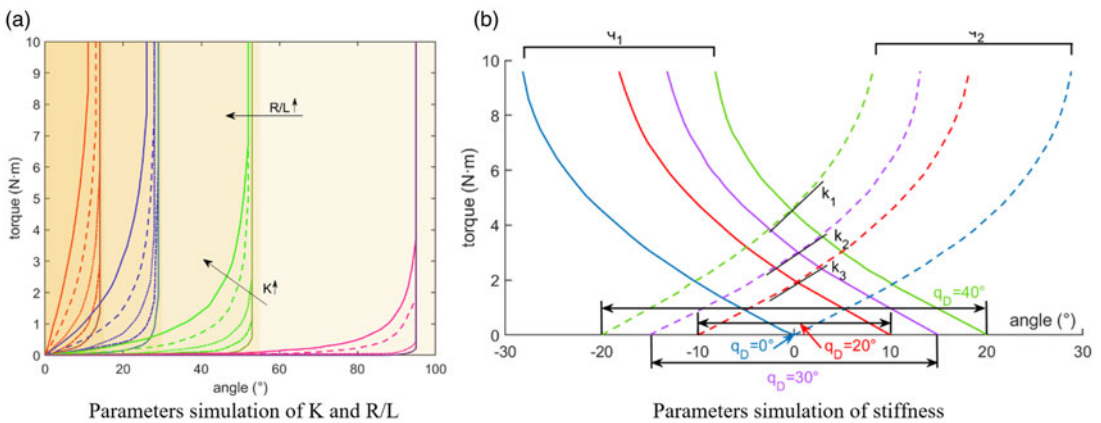


Figure 3. VSA parameter simulation. a) Parameters simulation of K and R/L. b) Parameters simulation of stiffness.

inputs, which rotates in opposite directions to generate antagonistic torque. In the symmetric structure composed of these two VSAs, the input angles of the two VSAs are set as the same q_1 . The rotation angle of the output bar is q_2 . Due to the symmetry of this VSA mechanism structure, when the stiffness of the left and right torsion springs is consistent, the output arm will be located in the balance position which follows the elbow muscle characteristic shown in Figure 1. Therefore, q_s can be used to control the desired angle position. And q_D can be used to control the output torque. As a result, the stiffness of VSA mechanism can be determined with q_s and q_D as shown in Figure 2.

When using the VSA mechanism to drive the elbow joint, parameters of the input wheel and output bar can influence the stiffness variation characteristic. The stiffness of the VSA mechanism is mainly related to three parameters: the radius R of input wheels; the length L of output bar and the stiffness K of elastic element. To ensure the output torque is stable, the stiffness K of a linear torsion spring and the ratio R/L should be optimized with simulation as shown in Figure 3a). It illustrates the relationship between exoskeleton torque and these three parameters. As the result shows, when K and R/L increase, the torque will also increase which has the same trend of stiffness variation. However, K and R/L are structural parameters that have been determined during the design and manufacturing process. The real-time variable stiffness control can only be achieved by changing the angles of q_s and q_D . Moreover, with the increment of q_D , the change of stiffness trends to be stable which will decrease the deviation between the actual stiffness and the ideal stiffness.

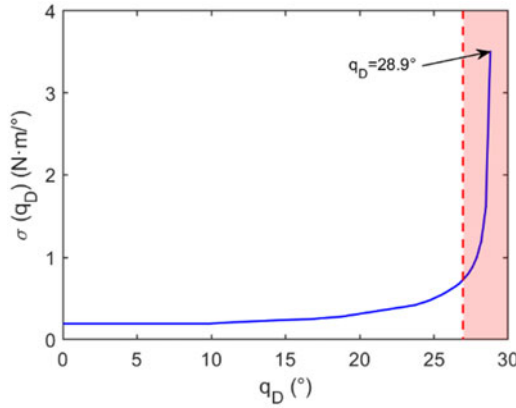


Figure 4. Stiffness analysis with q_D .

As a symmetric mechanism, the q_S is usually set to 0 when the elbow is stable. In that condition, we simulate the output torque with different q_1 and q_D . The variation of q_1 is 10° , 20° , and 30° while the q_2 is set symmetrically the same as q_1 . Respectively, q_D is set as 20° , 30° , and 40° . The output torque varies as shown in Figure 3b). Moreover, the slopes at the cross point of the dashed line are k_1 , k_2 , and k_3 which represent the corresponding stiffness values. Due to the symmetric actuation method in a balanced state, the output bar must locate at the balance position $q_S = 0^\circ$. As the same trend of our principle, the stiffness K increases with the rise of q_D .

As a result, the stiffness of VSA is controlled by controlling q_D , and the specific relationship is represented as follows:

$$\sigma(q_D) = \frac{1}{4}k \left[\left(\frac{4 \cos \frac{q_D}{4}}{\sqrt{1 - (4 \sin \frac{q_D}{4})^2}} - 1 \right)^2 + \frac{60 \cdot \beta \sin \frac{q_D}{4}}{\left[1 - (4 \sin \frac{q_D}{4})^2 \right]^{\frac{3}{2}}} \right] \tag{1}$$

Due to the structural limitations of the mechanism, when q_D approaches 28.93° , the stiffness k tends to infinity. Therefore, it is appropriate to limit q_D within $0\text{--}27^\circ$, and the range of stiffness variation is approximately $0.16\text{--}1 \text{ N}\cdot\text{m}/^\circ$ shown in Figure 4.

2.3 Structure design of variable stiffness actuator

Due to the high driving torque required for the elbow joint, the VSA mechanism should have a strong load-bearing capacity. At the same time, due to the size limitation of the elbow exoskeleton, the size of the VSA mechanism needs to be limited within an appropriate range. Based on the comprehensive analysis of these two points, a VSA mechanism based on a four bar linkage mechanism was designed as shown in Figure 5.

The VSA mechanism is composed of input unit, output unit, and transmission structure. Input unit including input wheel and axis is driven by Boden cable to q_1 . Output unit including output wheel and axis drives forearm to q_2 . Transmission structure including bearing, linkage and elastic element adjust the stiffness of VSA according to q_D . Two SEAs are set on the inner and outer side of elbow exoskeleton for symmetric actuation.

With the simulation above, we need to calculate the stiffness of VSA. After that, we select proper parameters of all parts. As the physiological structure shows, the motion parameters of elbow are shown in Table II.

As analysed in clinical training, to lift a person’s arm in a relaxed state, a torque of at least $3 \text{ N}\cdot\text{m}$ or more is required. Moreover, in active rehabilitation training, the elbow exoskeleton needs to provide

Table II. Elbow motion parameters.

Item	Unit	Value
Elbow angle	(°)	0~140 ± 10
Upper arm length	(mm)	301
Forearm length	(mm)	325
Forearm weight	(kg)	2.52
Elbow maximum torque	(N·m)	29.066
Maximum velocity	(°/s)	58

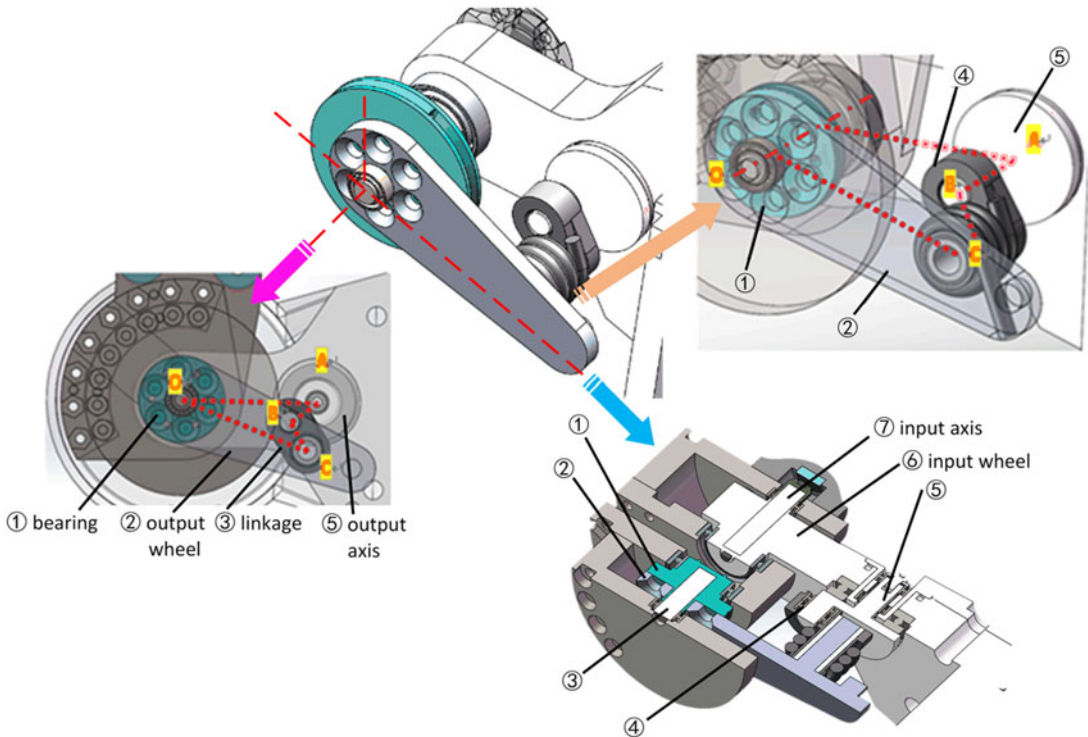


Figure 5. Structure design of VSA mechanism.

a torque of about 8 N · m in active rehabilitation training and a torque of about 10 N · m in passive rehabilitation training. Thus, we choose the output torque as 10 N · m for safety.

The calculation of the stiffness K of the torsion spring is as follows:

$$K = \frac{1 \times 0.0098 \times (19600 \times d^4)}{1167 \times (D - d) \times \pi \times N} \tag{2}$$

where d is the minor diameter, D is the major diameter, N is the number of spring coils.

To connect the output torque M and the output angle θ , the relationship is as follows:

$$M(\theta) = \frac{1}{2} K \beta \left(\frac{\frac{R}{L} \cos\left(\frac{\theta}{2}\right)}{\sqrt{1 - \left(\frac{R}{L} \sin\left(\frac{\theta}{2}\right)\right)^2}} - 1 \right) \tag{3}$$

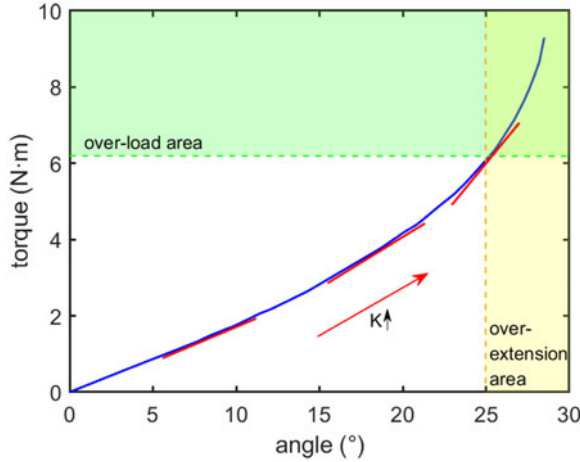


Figure 6. Design for elastic elements.

$$\beta = \arcsin\left(\frac{R}{L} \sin\left(\frac{\theta}{2}\right)\right) - \frac{\theta}{2} \tag{4}$$

After preliminary calculation, to meet the required requirements, the proposed spring parameters are as follows: $d = 2.5 \text{ mm}$, $D = 12 \text{ mm}$, $N = 3$. Finally, it can be concluded that $K = 0.0718 \text{ N} \cdot \text{m}^\circ$ as shown in Figure 6.

3. Deviation compensation unit design for elbow exoskeleton

3.1 Axis deviation simulation

The movement of elbow flexion and extension can be equivalent to a rotational motion around a cylindrical surface. However, its axis of rotation is not fixed because the humeral trochlear is not actually a standard cylindrical surface. Instead, the humeral trochlear is composed of two ellipsoidal surfaces with a groove in the middle to limit the lateral degrees of freedom of the joint. The range of motion of the joint axis is A_{ML} . When rotating, the angle between the central axis A_U of the forearm and the axis A_H of the humerus on the coronal plane is $80^\circ\text{--}92^\circ$. Moreover, the elbow joint axis will be accompanied by a displacement of -5 mm to 7 mm in the horizontal plane. The angle between two opposing elliptical spheres in the horizontal plane is 6° while an angle on the coronal plane is 10° .

In order to verify whether the passive compensation unit can compensate for the deviation of the elbow joint axis, we design a model with 5 degrees of freedom (DOF) to simulate the deviation motion of elbow axis as shown in Figure 7. To reduce the inappropriate torque and force caused by joint misalignment, the model simulates the possible movement of the elbow joint axis and examines the motion of the main passive compensation units.

The mechanism model contains 5 degrees of freedom, covering all possible motion scenarios of the human elbow joint axis. By adjusting the position of the elbow joint axis through the motion pair of the mechanism, it is possible to simulate the small displacement caused by elbow joint misalignment. With the deviation compensation unit, the exoskeleton allows the forearm to rotate away from the axis A_{ML} , which can avoid the secondary injury caused by the non-axial motion. Patients will feel less contact force and more comfortable with the deviation compensation unit.

3.2 Structure design of axis compensation unit

As shown in Figure 8a, we design an optimized linkage structure with four rotation pairs and two parallel sliding pairs to compensate for the 5 DOF axis deviation. After that, we design a deviation compensation

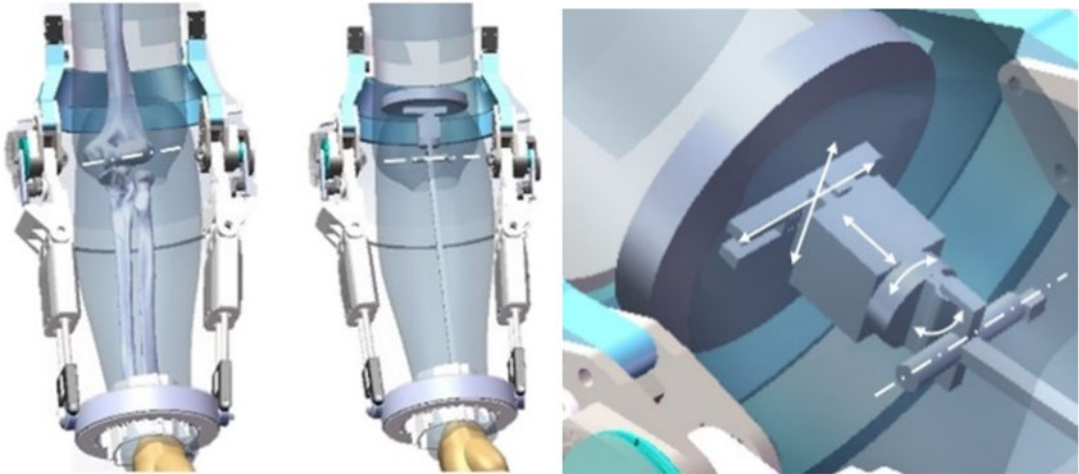


Figure 7. Axis deviation simulation.

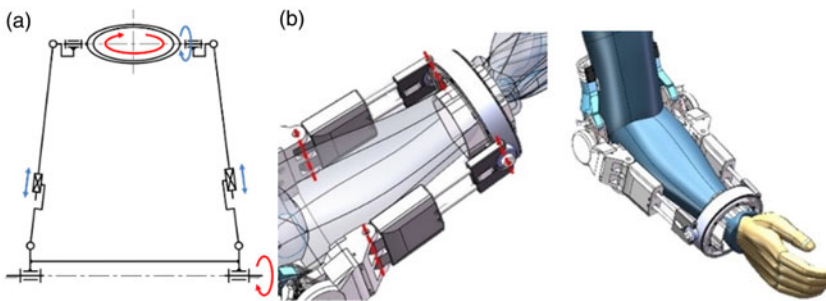


Figure 8. Structure design of deviation compensation unit. a) Linkage structure. b) Mechanism of compensation unit.

unit to meet the need of deviation compensation as shown in Figure 8b. The wrist joint part can be easily installed, and the motion of the deviation compensation unit can follow the motion of forearm passively.

When the translation range of the axis is in the horizontal plane, the motion of the translation deviation compensation unit is shown in Figure 9a. This compensation structure consists of four rotation pairs and two parallel sliding pairs. When the elbow joint axis moves forward through the combined effect of translation and rotation, the wrist is also moved forward. When the offset range of the axis within the horizontal plane $\beta_h = 6^\circ$, the motion of rotation compensation is shown in Figure 9b. When the elbow joint axis is offset within the coronal plane $\beta_i = 6^\circ$, it will cause the forearm to undergo a 6° spin motion. The motion of the coronal compensation unit is shown in Figure 9c, which can achieve passive compensation effect.

4. Simulation and experiment for elbow exoskeleton with variable stiffness actuator

4.1. Simulation of variable stiffness actuator

After selecting the stiffness characteristics of the VSA mechanism, it was applied to the dynamic simulation of actual rehabilitation process to test the influence of VSA mechanism stiffness on the rehabilitation process: setting q_D to 20° , 30° , and 40° . We simulate the process of exoskeleton to assist the patient's forearm to move from 130.2° to 60.2° in a relaxed state of human hands.

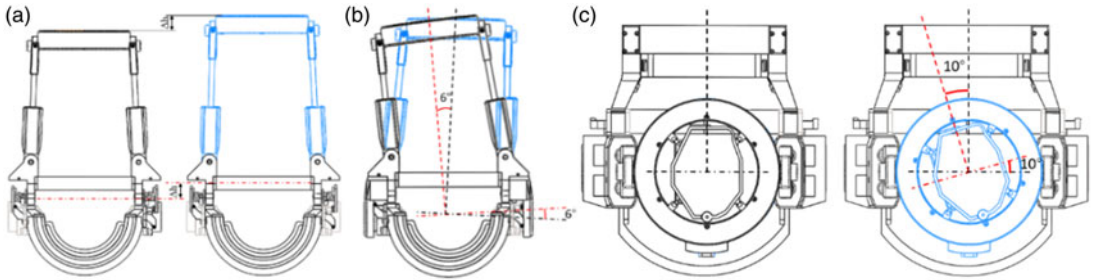


Figure 9. Validation of deviation compensation unit design. a) Translation compensation. b) Rotation compensation. c) Coronal compensation.

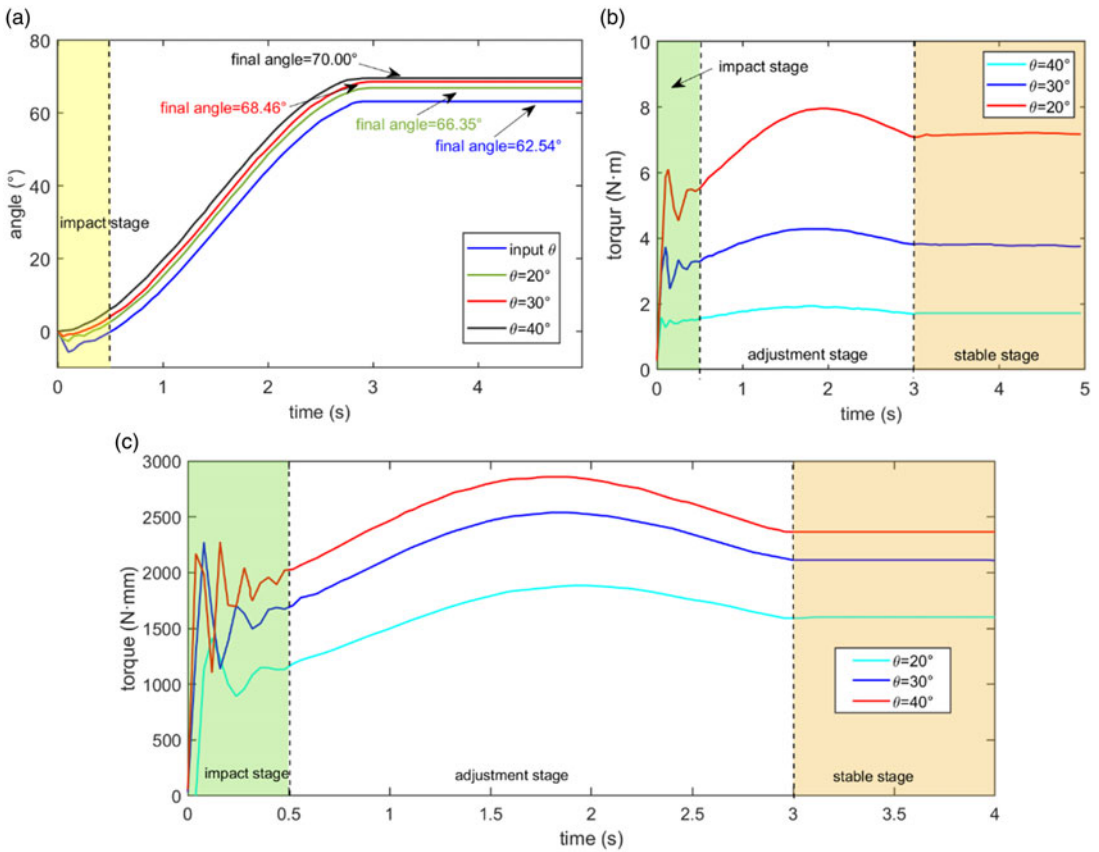


Figure 10. Elbow VSA simulation curve. a) Time-translation simulation curve. b) Time-rotation deviation simulation curve. c) Time-torque simulation curve.

In these three cases, the variation of elbow joint angular displacement with time was simulated separately in Figure 10 (a). With different expected output angle, our elbow exoskeleton can stably achieve the final angle after the impact stage.

After that, the output torque is simulated with the variation of input angle as shown in Figure 12b. The final torque can be adjusted with different input q_D . Moreover, the torque can meet the need of rehabilitation in the stable stage. Finally, the torque at the output wheel was obtained in three different

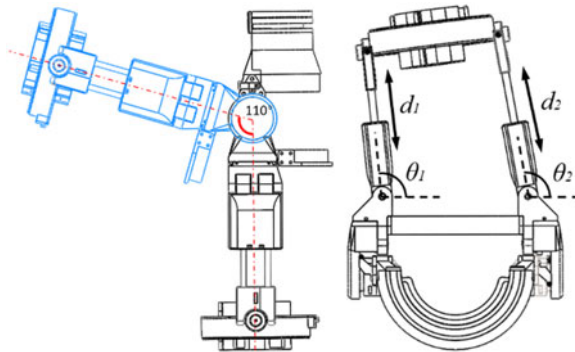


Figure 11. Simulation parameters of deviation compensation unit.

scenarios in Figure 12c. The final torque can be adjusted with different input q_s . The torque varies at different balance points which accords with the physiological analysis in Figure 1.

It can be seen that as the angle q_D of the VSA mechanism on both sides increases, the stiffness increases, and the angle in Figure 12a follows better with less difference. But in Figure 12b and c, this stiffness causes some oscillations. The larger the stiffness is, the more the oscillations pronounced. When $q_D = 40^\circ$, the peak torque is about $2.85 \text{ N} \cdot \text{m}$. Therefore, the stiffness of the elbow exoskeleton can be changed at any time by controlling the size of q_D to meet the needs of patients in various stages of rehabilitation.

4.2 Simulation of deviation compensation unit

After VSA simulation, we simulate the motion, torque, and force of deviation compensation unit during the rehabilitation process. Starting from the natural relaxation state of the human elbow, the swinging range is from 0° to 110° under the drive of our exoskeleton. The simulation frequency is 1 Hz, and the simulation duration is 20s. The compensation motion of the rotation and translation joints, as well as the force and torque of the human wrist, are measured to determine whether it can reduce the inappropriate torque of the wrist. As Figure 11 shows, the deflection and translation of the four key passive joints are simulated when the exoskeleton swings at 1 Hz within the range of motion from 0° to 110° .

The force and torque in three dimensions of the wrist are shown. F_z is the main force used to lift the patient's forearm. Other forces F_x , F_y , and torques M_x , M_y , M_z are all harmful and not desirable. Moreover, the effectiveness of the deviation compensation unit can be determined by detecting the magnitude of these forces and torques. As the results shown in Figure 12, the maximum torque applied on the wrist is $0.114 \text{ N} \cdot \text{m}$, while the maximum force applied is about 4.5 N . Those two factors, especially torque can cause secondary injuries on the elbow. With our deviation compensation unit, the inappropriate torque and force are in acceptable range. Both the torque and force can meet the patient's comfort requirements.

4.3 Tests of elbow exoskeleton in rehabilitation platform

The rehabilitation platform of the elbow exoskeleton mainly includes the elbow exoskeleton, driving motor, hardware equipment, and angle sensors as shown in Figure 13. The elbow robot is installed on the chair platform, and the motor and other hardware equipment are located on the bottom plate of the chair. The motor transmits the driving force along the Bowden cable from the motor end to the elbow exoskeleton. The control board at the bottom plate is directly connected to the slave (Microcomputer, MC). Our elbow exoskeleton motion is controlled through the host (Personal Computer, PC).

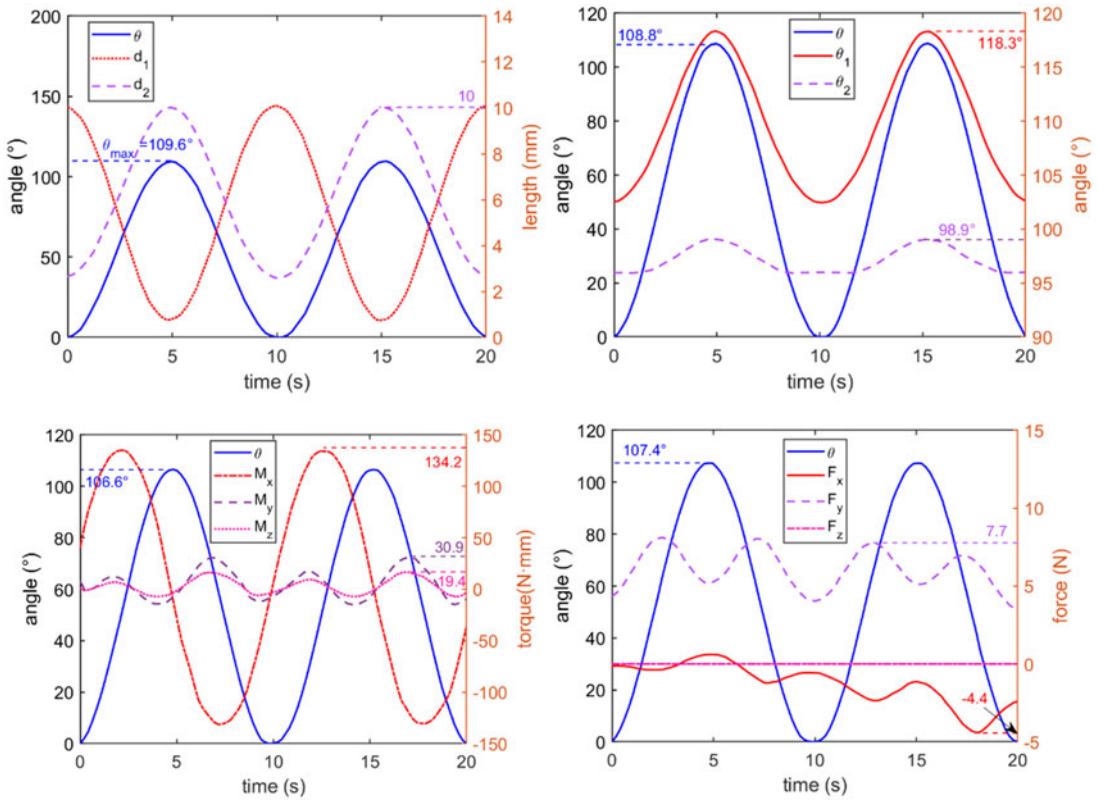


Figure 12. Deviation compensation unit simulation.

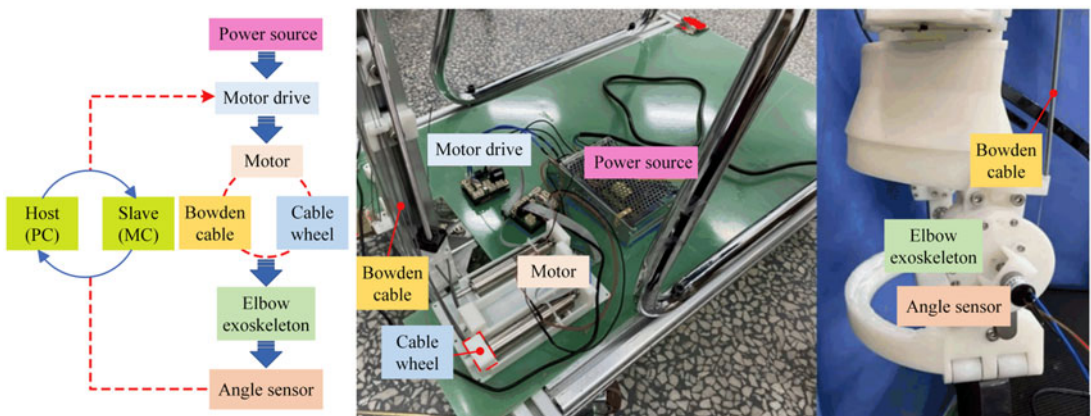


Figure 13. Elbow exoskeleton experiment platform.

Good wearability is one of the design requirements for exoskeleton, which requires the size of the exoskeleton to match the dimensions of relevant parts of the human upper limbs. It should be convenient for patients to quickly wear and remove. As shown in Figure 14 and Figure 15, the flexion/extension and pre/post-rotation degrees of freedom of the elbow joint are tested. The joint angle changes during rehabilitation. The angle ranges of each degree of freedom during the exercise are recorded in Table II.

Table III. Elbow motion parameters.

DOF of elbow	Maximum ROM		
	Human	Rehabilitation demand	Elbow robot
Spin forward/back	-90°~ +90°	-80°~ +80°	-85°~ +85°
Flexion/extension	-10°~+140°	0°~110°	0°~140°

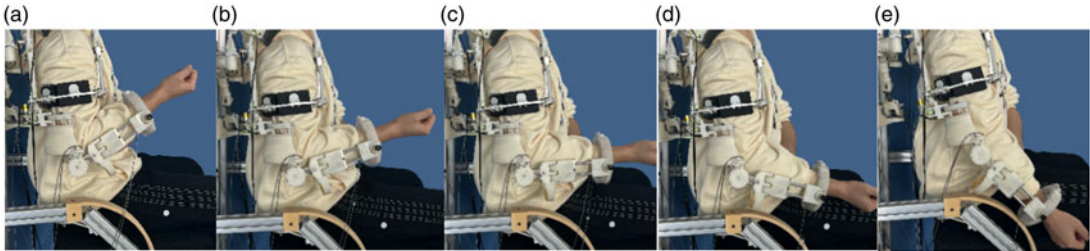


Figure 14. Flexion/extension motion test.

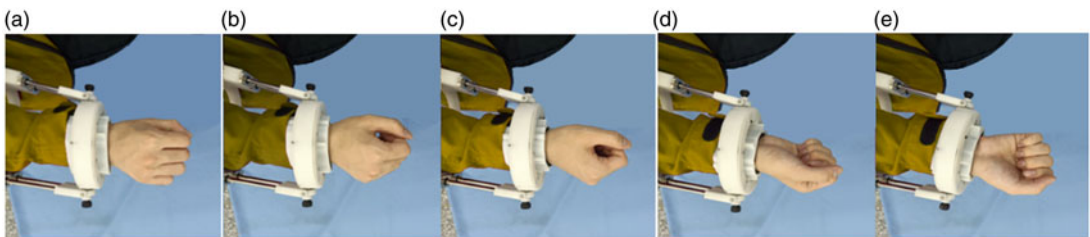


Figure 15. Spin forward/back motion test.

The experimental results in Table III indicate that the range of motion of each exoskeleton motion can meet the rehabilitation requirements. In addition, the elbow joint flexion and extension degrees of freedom also have an angle limiting which can prevent exoskeleton from exceeding the maximum range of elbow angles.

The flexion/extension movement of the elbow joint is a key focus in rehabilitation training. This experiment tested the curve of the flexion/extension movement of the exoskeleton elbow joint under motor drive at different speeds and motion ranges. The following motion curves show that the maximum velocities of elbow joint are between 30°/s and 48°/s. The maximum range of motion (ROM) is 60°, 90°, and 120° respectively as shown in Figure 16.

Backlash as an ignorable factor affects the motion accuracy which should be tested and compensated. Moreover, for the VSA principle, the accuracy of stiffness is also influenced by backlash. Thus, we carry out the following experiments to measure the backlash within different ranges of elbow flexion motion shown in Figure 17.

During the rehabilitation training process, the output torque of the elbow exoskeleton can directly show the assistance and reflect the change of stiffness. According to the analysis results of the simulation, q_D is the key factor affecting stiffness: the larger q_D is, the larger the stiffness is. We carry out an experiment to control the stiffness by q_D . The joint torque curves are tested for one cycle of joint movement within the range of 0–110° at q_D of 10°, 15°, and 20°. The test results of stiffness variation and torque-flexion relationship are shown in Figure 18.

From the comparison of the three curves, as the stiffness increases, the maximum torque required to drive elbow joint also increases. This is because the stiffness is related to the pre-tightening force of the Bowden cable. As the stiffness increases, the pre-tightening force of the Bowden cable increases,

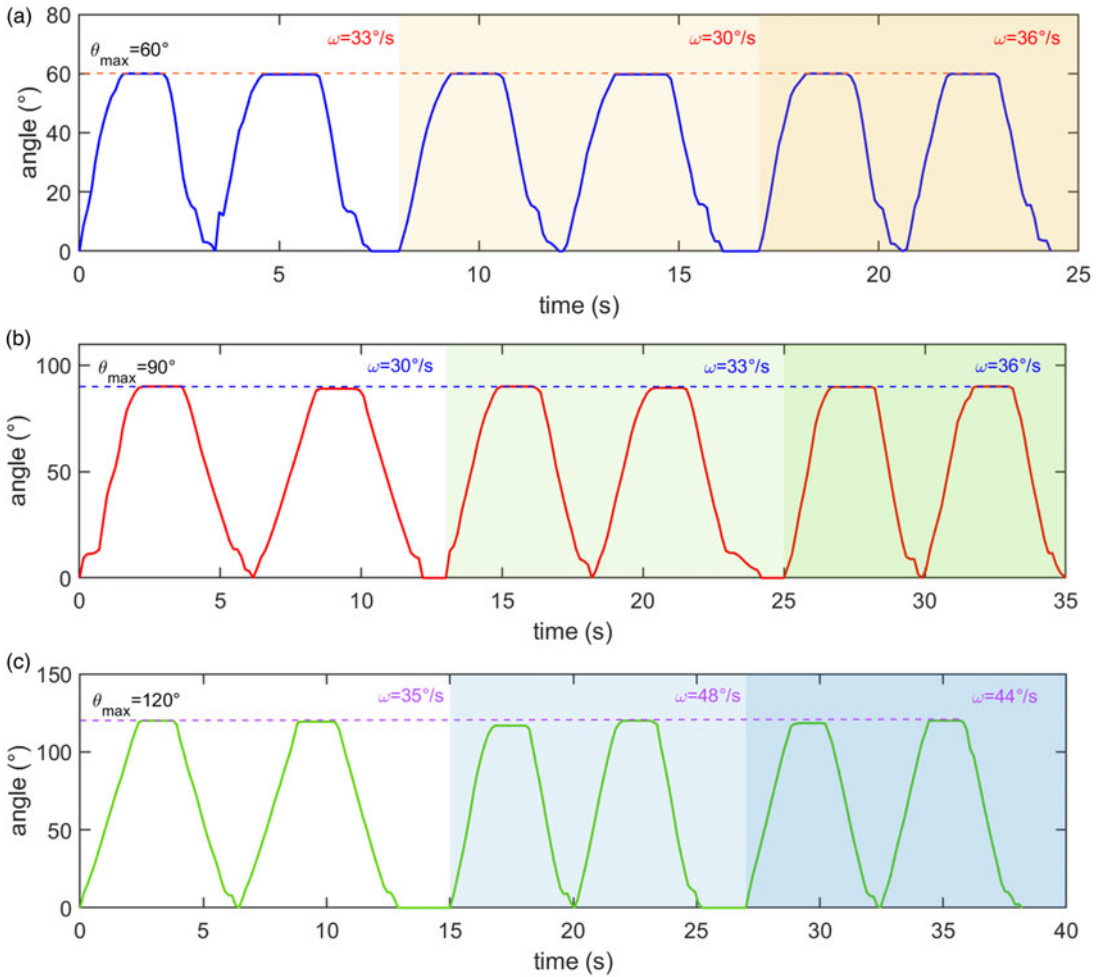


Figure 16. Flexion/extension motion reputation test. a) Maximum ROM at 60°. b) Maximum ROM at 90°. c) Maximum ROM at 120°.

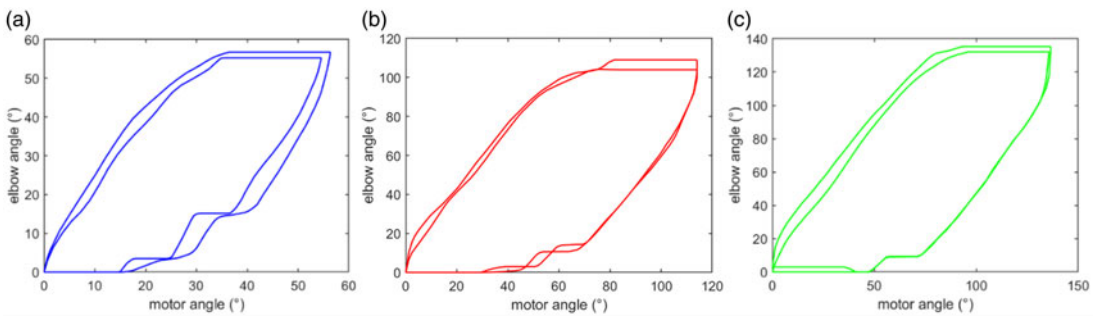


Figure 17. Backlash test. a) Backlash at 60°. b) Backlash at 115°. c) Backlash at 140°.

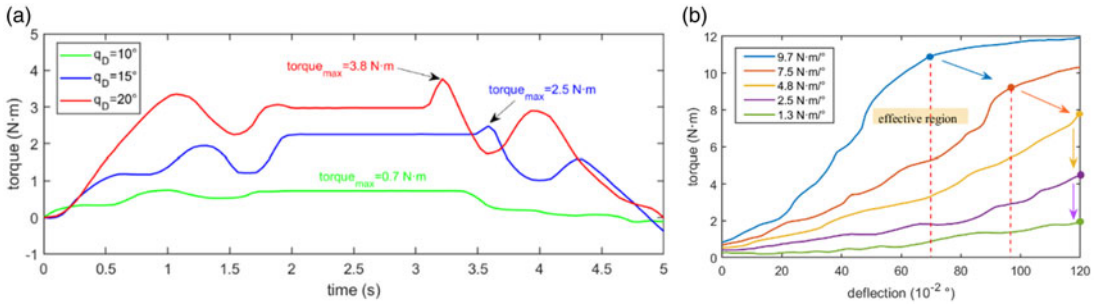


Figure 18. Variable stiffness test. a) Stiffness variation test. b) Torque-flexion test.

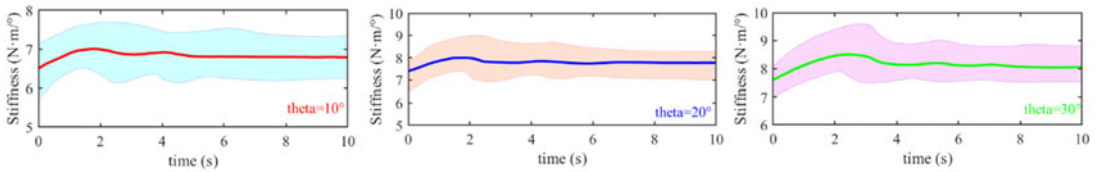


Figure 19. Stiffness adjustment test.

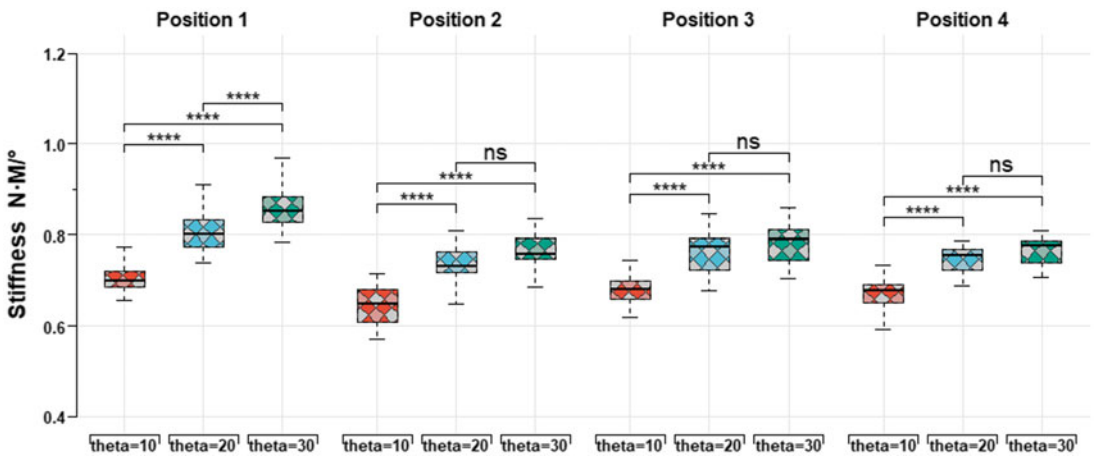


Figure 20. Stiffness analysis.

leading to greater friction in the intermediate linkage and an increased torque for actuation. In addition, oscillations occurring between 3 and 4 s can be clearly observed, mainly due to the inertia of the mechanism when the motor suddenly starts and stops. As the stiffness increases, the oscillation becomes more pronounced.

Moreover, we carry out an experiment and set q_D to 10° , 20° , and 30° . The result of stiffness adjustment is shown in Figure 19. We choose four positions as observation points and analysed the result of 60 times test. The result of stiffness change is shown in Figure 20. After that, we compare the simulation results and the experiment. The deviations of stiffness are 0.12 ± 0.03 N·m/°, 0.16 ± 0.08 N·m/° and 0.15 ± 0.05 N·m/°, respectively to 10° , 20° , and 30° . With the increment of q_D , the accuracy of stiffness adjustment increases as we simulated above. From the results, we can see that our elbow rehabilitation robot can achieve a 0–140° ROM with 30–48°/s velocity. The stiffness can be adjusted from 0.48 N·m/° to 0.79 N·m/° as shown in Figure 21. The performance of our exoskeleton can not only satisfy the needs

Type of robot	Reference	Type of drive	Compensation mechanism	Variable stiffness	ROM	Speed	Stiffness
Elbow robot	Ours	●	▲	■	0-140°	30-48°/s	4.8-9.7 N·m/°
Elbow robot	[4]	●	▲	■	-	-	-
Upper limb robot	[13]	●	▲	■	60-180°	30°/s	-
Elbow robot	[15]	●	▲	■	90-157°	-	-
Upper limb robot	[16]	●	▲	■	-	-	-
Upper limb robot	[17]	●	▲	■	0-150°	-	-
Elbow robot	[18]	●	▲	■	0-93°	38°/s	47.9 N/mm
Elbow robot	[19]	●	▲	■	0-120°	7-16°/s	-
Upper limb robot	[20]	●	▲	■	0-135°	91°/s	1.68-5.63 N·m/°
Elbow robot	[24]	●	▲	■	70-180°	10-27°/s	1.01 N/mm
Elbow robot	[25]	●	▲	■	0-95°	-	0.17-0.73 N·m/°
Upper limb robot	[27]	●	▲	■	0-145°	-	-
Elbow robot	[30]	●	▲	■	0-120°	-	24-56 N·m/rad

Variable stiffness

- ADCJ
- Adjusting cable
- Not designed
- Pressure dependent
- VSA

Compensation mechanism

- ▲ Not designed
- ▲ Parallel mechanism
- ▲ Passive mechanism
- ▲ Slider crack
- ▲ Soft exoskeleton
- ▲ Spherical mechanism

Type of drive

- Cable drive
- Hybrid drive
- Hydraulic drive
- Motor drive

Figure 21. Performance of our elbow rehabilitation robot.

of elbow rehabilitation but also provide a comfortable and safe rehabilitation progress with variable stiffness.

5. Conclusion

The increasing demand of elbow rehabilitation proposes requirements for assistance with elbow exoskeleton. The introduction of elbow exoskeleton can help improve the patients’ motion function with the guidance of therapists. In this paper, an elbow exoskeleton is designed with adjustable stiffness and compensation unit to assist elbow rehabilitation.

- 1) A variable stiffness actuator based on symmetric actuation principle is studied. To simulate the parameters, the exoskeleton stiffness can be adjusted by changing the ratio of output angle to deviation angle. The adjustable stiffness can fit the human elbow stiffness in rehabilitation.
- 2) Based on the physiological analysis of elbow axis motion, the axis deviation is fitted with a design of deviation compensation unit. A parallel sliding mechanism with 5 DOF can follow the axis deviation outside the horizontal plane. With the optimization of mechanism parameters, the range of motion can meet the compensation requirement. The additional torque can be reduced to 0.114 N·m and the contact force can be reduced to 4.5N.
- 3) Experiments are carried out with our rehabilitation platform to show the performance of our elbow exoskeleton. The stiffness of our elbow exoskeleton can be adjusted from 0.48N·m/° to 0.97N·m/°. The maximum range of spinning forward/back and flexion/extension can be up to -85°~+85° and 0°~140° respectively.
- 4) For cable-driven exoskeleton, a backlash test is carried out to increase the control accuracy of motion and stiffness.

Author contributions. Lei Yang and Fuhai Zhang conceived and designed the study. Lei Yang performed experiments. Lei Yang, Fuhai Zhang, and Yili Fu wrote the article.

Financial support. This work was supported in part by the National Natural Science Foundation of China under Grant 62073097; in part by the Natural Science Foundation of Heilongjiang Province of China under Grant LH2021F027; and in part by the State Key Laboratory of Robotics and System, Harbin Institute of Technology (HIT), under Grant SKLRS202107B.

Competing interests. The authors declare no competing interest exists.

Ethical approval. Not applicable.

References

- [1] M. Cao and X. Li, “Effectiveness of modified constraint-induced movement therapy for upper limb function intervention following stroke: A brief review,” *Sports Med. Health Sci.* **3**(3), 134–137 (2021).
- [2] A. Shumway-Cook and M. H. Woollacott. *Motor Control: Translating Research into Clinical Practice*. 5th edition, (Lippincott Williams & Wilkins, USA, 2016).
- [3] J. Laut, M. Porfiri and P. Raghavan, “The present and future of robotic technology in rehabilitation,” *Curr. Phys. Med. Rehab. Rep.* **4**(4), 312–319 (2016).
- [4] D. H. de la Iglesia, A.S. Mendes, G.V. González, D.M. Jiménez-Bravo and J. F. de Paz Santana, “Connected elbow exoskeleton system for rehabilitation training based on virtual reality and context-aware,” *Sensors* **20**(3), 858 (2020).
- [5] L. Lin, F. Zhang, L. Yang and Y. Fu, “Design and modeling of a hybrid soft-rigid hand exoskeleton for poststroke rehabilitation,” *Int. J. Mech. Sci.* **212**, 106831 (2021).
- [6] H.M. Qassim and W. Z. Wan Hasan, “A review on upper limb rehabilitation robots,” *Appl. Sci.* **10**(19), 6976 (2020).
- [7] L. Maria, M. Andrea, P. Paolo, et al., “Instrumental indices for upper limb function assessment in stroke patients: A validation study,” *J. Neuroeng. Rehabil.* **52**(13), 1–11 (2016).
- [8] C. M. Dean, C. Rissel, S. Sherrington, M. Sharkey, R. G. Cumming, S. R. Lord, R. N. Barker, C. Kirkham and S. O’Rourke, “Exercise to enhance mobility and prevent falls after stroke: The community stroke club randomized trial,” *Neurorehabil. Neural Repair* **68**(9), 1046–1057 (2012).
- [9] A.H. Korayem, S.R. Nekoo and M. H. Korayem, “Optimal sliding mode control design based on the state-dependent Riccati equation for cooperative manipulators to increase dynamic load carrying capacity,” *Robotica* **37**(2), 321–337 (2019).
- [10] L. A. Ingram, A. A. Butler, L. D. Walsh, M. A. Brodie, S. R. Lord, S. C. Gandevia and F. Tremblay, “The upper limb physiological profile assessment description, reliability, normative values and criterion validity,” *PLoS ONE* **14**(6), 1–33 (2019).
- [11] B. D. M. Chaparro-Rico, C. Daniele, et al., “NURSE-2 DoF device for arm motion guidance: Kinematic, dynamic, and FEM analysis,” *Appl. Sci.* **10**(2139), 1–22 (2020).
- [12] T.-Y. Shih, C.-Y. Wu, K.-C. Lin, C.-H. Cheng, Y.-W. Hsieh, C.-L. Chen, C.-J. Lai and C.-C. Chen, “Effects of action observation therapy and mirror therapy after stroke on rehabilitation outcomes and neural mechanisms by MEG: Study protocol for a randomized controlled trial,” *Trials* **18**(1), 459 (2017).
- [13] T. Proietti, C. O’Neill, C. J. Hohimer, K. Nuckols, M. E. Clarke, Y. M. Zhou, D. J. Lin and C. J. Walsh, “Sensing and control of a multi-joint soft wearable robot for upper-limb assistance and rehabilitation,” *IEEE Robot. Autom. Lett.* **6**(2), 2381–2388 (2021).
- [14] F.H. Zhang, L. Yang and Y. L. Fu, “Design of a novel elastic torque sensor for hand injuries rehabilitation based on bowden cable,” *IEEE Trans. Instrum. Meas.* **68**(9), 3184–3192 (2019).
- [15] I. Rifky, A. Mochammad, I. A. Perkasa et al., “Soft elbow exoskeleton for upper limb assistance incorporating dual motor-tendon actuator,” *Electronics* **8**(10), 1184 (2019).
- [16] R. Ma, Z. Tang, X. Gao, et al. “Mechanism Design and Kinematics Analysis of an Original Cable-driving Exoskeleton Robot”, *In: 2018, 2nd IEEE Advanced Information Management, Communicates, Electronic and Automation Control Conference (IMCEC)*, (2018) pp. 1869–1874.
- [17] J. C. Perry, J. Rosen and S. Burns, “Upper-limb powered exoskeleton design,” *IEEE/ASME Trans. Mechatron.* **12**(4), 408–417 (2007).
- [18] K.Y. Wu, Y.Y. Su, Y.L. Yu, et al. “Series Elastic Actuation of an Elbow Rehabilitation Exoskeleton with Axis Misalignment Adaptation”, *In: 2017 International Conference on Rehabilitation Robotics (ICORR)*. *IEEE Int Conf Rehabil Robot*, (2017) pp. 567–572.
- [19] D. Copaci, F. Martin, L. Moreno and D. Blanco, “SMA based elbow exoskeleton for rehabilitation therapy and patient evaluation,” *IEEE Access* **7**, 31473–31484 (2019).
- [20] M. Dežman, T. Asfour, A. Ude, et al., “Mechanical design and friction modelling of a cable-driven upper-limb upper limb exoskeleton,” *Robotica* **39**(9), 1711–1728 (2021).
- [21] Y. Fan, J. Yuan, Y. Wu and H. Qiao, “A feedforward compensation approach for cable-driven musculoskeletal systems,” *Robotica* **41**(4), 1221–1230 (2023).
- [22] J.F. Rodríguez-León, B. D. M. Chaparro-Rico, M. Russo and D. Cafolla, “An autotuning cable-driven device for home rehabilitation,” *J. Healthc. Eng.* **2021**, 1–15 (2021).
- [23] W. Saab, W. Rone and P. Ben-Tzvi, “Discrete modular serpentine robotic tail: Design, analysis and experimentation,” *Robotica* **36**(7), 994–1018 (2018).
- [24] Q. Wu, B. Chen and H. Wu, “Neural-network-enhanced torque estimation control of a soft wearable exoskeleton for elbow assistance,” *Mechatronics* **63**, 102279 (2019).
- [25] T. Chen, R. Casas and P. S. Lum, “An elbow exoskeleton for upper limb rehabilitation with series elastic actuator and cable-driven differential,” *IEEE Trans. Robot.* **35**(6), 1464–1474 (2019).
- [26] I. Jakob, A. Kollreider, M. Germanotta, F. Benetti, A. Cruciani, L. Padua and I. Aprile, “Robotic and sensor technology for upper limb rehabilitation,” *PM&R* **10**(9), 189–197 (2018).
- [27] M. R. Islam, M. Rahmani and M. H. Rahman, “A novel exoskeleton with fractional sliding mode control for upper limb rehabilitation,” *Robotica* **38**(11), 2099–2120 (2020).

- [28] V. Klamroth-Marganska, J. Blanco, K. Campen, A. Curt, V. Dietz, T. Ettl, M. Felder, B. Fellinghauer, M. Guidali, A. Kollmar, A. Luft, T. Nef, C. Schuster-Amft, W. Stahel and R. Riener, “Three-dimensional, task-specific robot therapy of the arm after stroke: A multicentre, parallel-group randomised trial,” *Lancet Neurol.* **13**(2), 159–166 (2014).
- [29] D. Verdel, S. Bastide, N. Vignais, O. Bruneau and B. Berret, “An identification-based method improving the transparency of a robotic upper limb exoskeleton,” *Robotica* **39**(9), 1711–1728 (2021).
- [30] N. Vitiello, T. Lenzi, S. Roccella, S. M. M. De Rossi, E. Cattin, F. Giovacchini, F. Vecchi and M. C. Carrozza, “NEUROExos: A powered elbow exoskeleton for physical rehabilitation,” *IEEE Trans. Robot.* **29**(1), 220–235 (2013).